

CHALMERS



Experimental Study of Air Flow in a Hydro Power Generator Model

Design, Construction and Measurements

Master's Thesis in Solid and Fluid Mechanics

ERWIN ADI HARTONO

Department of Applied Mechanics

Division of Fluid Dynamics

CHALMERS UNIVERSITY OF TECHNOLOGY

Göteborg, Sweden 2011

Master's Thesis 2011:51

MASTER'S THESIS 2011:51

Experimental Study of Air Flow in a Hydro Power Generator Model

Design, Construction and Measurements

Master's Thesis in Solid and Fluid Mechanics
ERWIN ADI HARTONO

Department of Applied Mechanics
Division of Fluid Dynamics
CHALMERS UNIVERSITY OF TECHNOLOGY
Göteborg, Sweden 2011

Experimental Study of Air Flow in a Hydro Power Generator Model
Design, Construction and Measurements
ERWIN ADI HARTONO

©ERWIN ADI HARTONO, 2011

Master's Thesis 2011:51
ISSN 1652-8557
Department of Applied Mechanics
Division of Fluid Dynamics
Chalmers University of Technology
SE-412 96 Göteborg
Sweden
Telephone: + 46 (0)31-772 1000

Cover:
The Experimental Rig

Chalmers Reproservice
Göteborg, Sweden 2011

Experimental Study of Air Flow in a Hydro Power Generator Model
Design, Construction and Measurements
Master's Thesis in Solid and Fluid Mechanics
ERWIN ADI HARTONO
Department of Applied Mechanics
Division of Fluid Dynamics
Chalmers University of Technology

Abstract

Air cooled electric generators have been studied for a long time, but there is still a lack of knowledge about the details of the air flow in such machinery.

In this work, a generator ventilation model was specially designed and constructed as a 1:2 model of an existing generator model in Uppsala University. Full flow Reynolds number similarity is achieved by increasing the rotation speed of the model generator. The rotor and the stator were built with rapid-prototyping techniques that could resolve the complex geometry with high accuracy. The manufacturing process also allows the inclusion of pressure taps, making it possible to measure the wall static pressure in the most interesting region. A sector of the stator was built in plexi-glass for the PIV measurements.

Six configurations were investigated: two different stators with three different rotor fan blades. The rotational speed was kept constant for all cases to maintain the same Reynolds number. The static pressure at the stator coils, stator inner and outer walls, and the total pressure at the outlet of the stator channels were measured.

Pressure transducer together with scanivalve were used to measure the static pressure around the coil. A custom made rake was built to measure the total pressure at the outlet of the channel. Mass flow was estimated by integrating the total pressure data from the outlet. Two static pressure taps at the top of enclosure wall was made to estimate the flow angles.

Around the coil the air flow has a large tangential component when entering the stator channels. The air flow was estimated to be swirl due to high flow angle. The static pressure at the stator inner wall increases as the air flows axially in the space between the rotor and stator. Half of the stator cooling channel was occupied by recirculation region. Estimated mass flow has approximately half the value compared to numerical calculation of 100% scale generator in Uppsala in accordance with design expectations.

Keywords: Experimental, Hydro Power, Generator, Air-Flow

Contents

Abstract	I
Contents	III
Preface	V
Acknowledgements	VI
Notations	VII
1 Introduction	1
1.1 Background	1
1.2 Purpose	1
1.3 Design Consideration	1
1.4 Previous Studies	3
1.5 Limitations	4
2 The Experimental Rig	5
2.1 General Overview	5
2.2 The Rotor	6
2.3 The Stator	6
2.4 The Fan Blades	7
2.5 The Top Lid	8
2.6 The Enclosure	9
2.7 The Shaft	9
2.8 The Experimental Rig Support Structure	10
3 Methodology	11
3.1 Static Pressure Measurement	11
3.2 Total Pressure Measurement	14
3.3 Mass Flow Estimation	15
3.3.1 Flow Angle Estimation From Static Pressure Measurement at The Enclosure	16
3.4 Error Estimation	18
4 Results and Discussion of the Pressure Measurement	19
4.1 Static Pressure Measurements Around The Stator Coils and Outlet of the Stator Channel	19
4.2 Static Pressure Measurements at Stator Walls, Inner and Outer . . .	19
4.3 Total Pressure Measurement at The Outlet of Stator Cooling Chan- nel with Total Pressure Rake	20

4.4	Mass Flow Estimation from Total Pressure Measurement at The Stator Cooling Channel	20
4.5	Flow Angle Estimation From Static Pressure Measurement at the Enclosure	20
4.6	Error Estimation	21
5	Conclusions	25
6	Future Work	26
A	Appendix: Periodicity of The Flow	28
B	Appendix: CAD Drawings	30
B.1	Rotor	31
B.2	Stator Curved Baffles 1 of 3	32
B.3	Stator Curved Baffles 2 of 3	33
B.4	Stator Curved Baffles 3 of 3	34
B.5	Stator Straight Baffles 1 of 3	35
B.6	Stator Straight Baffles 2 of 3	36
B.7	Stator Straight Baffles 3 of 3	37
B.8	Short fan blade	38
B.9	Medium fan blade	39
B.10	Long fan blade	40

Preface

This report contains two major parts. The first part describes the design and the construction of the components of the experimental rig. The second part describes the results from pressure measurement. The construction of the experimental rig was started in January 2011 and finished in June 2011. The measurements were done during summer 2011.

Acknowledgements

First of all I would like to thank God and my parents, Hartono Hadiprayitno and Cecilia Maria Tjitraningsih. There is no word to describe their kindness to me.

I would like to thank Ångpanneföreningens Forskningsstiftelse for the funding. Also VG Power for feedback on the design.

I also would like to thank my supervisors and the department of Applied Mechanics for their support;

- Håkan Nilsson, my first supervisor. Thank you for considering me as an appropriate person for this master thesis project.
- Valery Chernoray, my second supervisor. Thank you for helping me building the rig and for teaching me how to do experimental work.
- Pirooz Moradnia, my third supervisor. Thank you for the ride and for short discussion about future plan after master.

Also thanks to the manufacturers and the suppliers;

- Brion AB, who manufactured the plexi-glass parts.
- Combustion Workshop, Chalmers, for the shaft and its components.
- ACRON, for the stator.
- VOLVO, for the rotor.
- Flexlink, for the aluminium profile.
- Tools Momentum, for the bearing.
- Stalhandlarna, for the shaft.
- RB Plast & Glass, for the acrylic table.
- and others who helped me assembled the experimental rig.

The last but not least, for all my friends, Indonesian and non-Indonesian. I'm sorry guys, I cannot mention you one by one. All of you are important for me. Thank you very much.

Göteborg October 2011
Erwin Adi Hartono

Nomenclature

α	Flow angle
Δx	Distance between pipes of the rake
\dot{m}	Mass flow
ρ	Air density
A	Area
h	Distance between top lid and enclosure
N	Number of samples
p	Pressure
r	Radius
std	Standard deviation
t	Stator cooling channel height
V	Absolute velocity
v	Velocity components in radial direction
w	Velocity components in tangential direction

1 Introduction

1.1 Background

The total electric power production by the hydro power generators in Sweden is about 16.200 MW, which corresponds to approximately 45% of the total electricity produced in Sweden.

Today, the activity within the Swedish hydro power business is mostly limited to refurbishments and maintenance work [1]. In order to increase the performance, understanding of the problem is the key. One problem in generators is heat generation. Although generators have been cooled by air for a century, there is still a lack of knowledge of the air flow inside generators. This means that if the air flow inside the generators is fully understood, modifications can be performed to increase the overall performance through maintaining its optimum temperature operating condition and by minimizing the losses.

1.2 Purpose

The purpose of the present work is to build a scale model generator and study the air flow inside it. Pressure based measurements and laser based measurements will be used to study the air flow. The results are then considered as a database for comparison with numerical simulations. Thus, some request from numerical point of view has been taken into account in the design phase.

The model is based on a small-scale research generator located at Uppsala University, Sweden, which was built mainly for studying the electromagnetic fields in a generator. In the Uppsala generator model there are many obstacles for performing detailed measurements of the air flow, and also almost impossible to use optical methods while keeping electric functionality, as seen in figure 1.1. The generator at Uppsala University is therefore has restricted possibility of fluid mechanical measurements.

1.3 Design Consideration

Some consideration has been made in order to meet the requirement of experimental fluid dynamic point of view. Figure 1.2 shows the schematic view of the Uppsala University generator model.

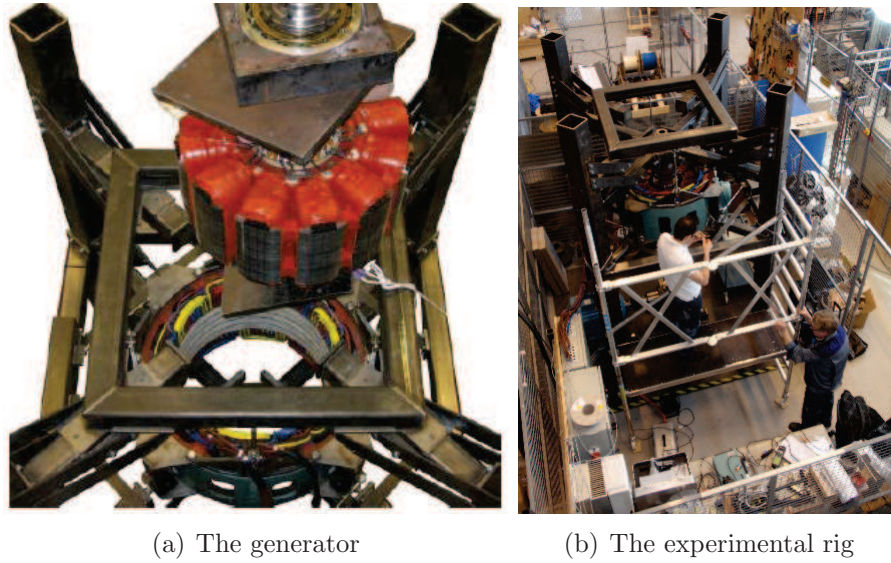


Figure 1.1: Uppsala university generator model. From Moradnia et al. [2]

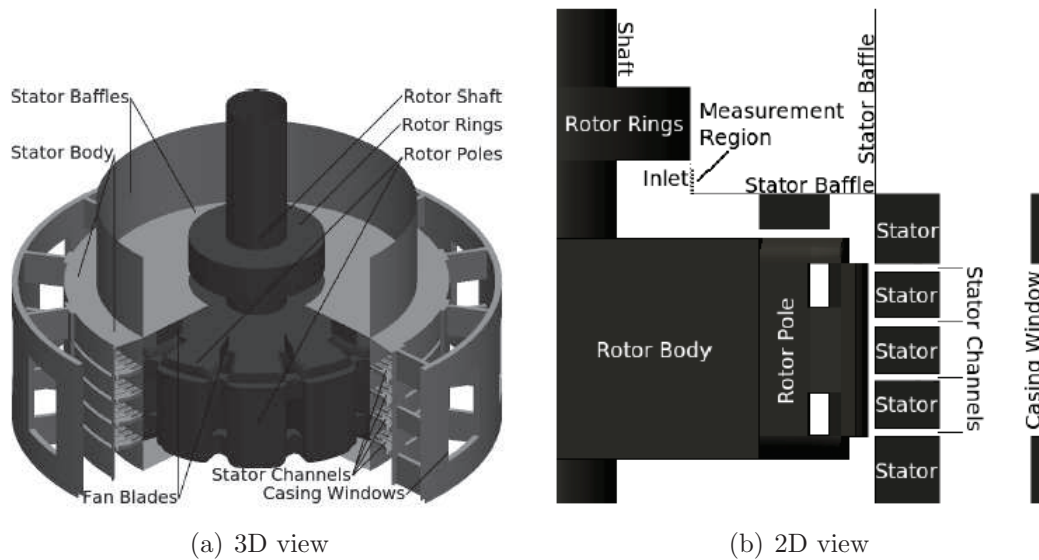


Figure 1.2: Schematic view of Uppsala University generator model. From Moradnia et al. [2]

Figure 1.3 shows the comparison between the Uppsala and the generator model that is used in this work. Some part is changed and replaced. In present work the casing windows is replaced with the enclosure, the 2 stator baffles are replaced with the top lid, the rotor ring is removed, and the fan is modified.

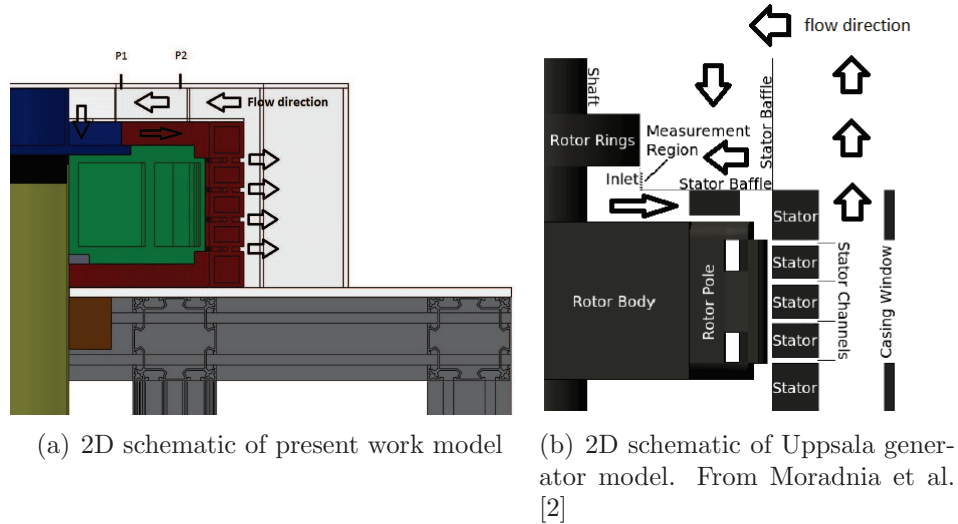


Figure 1.3: Chalmers and Uppsala university generator model

Rotor and stator is simplified for numerical fluid dynamics point of view. The rotor is built with SLS, selective laser sintering, technique. This technique is chosen due to SLS can produce relatively strong and ductile structure. Another rapid prototyping technique (SLA, Stereolithography Aparatus) is chosen for the stator. It is because the stator should have smooth surface and air tight, due to the pressure pipes were embedded inside the stator body. A new stator channel design, i.e. straight channel, is designed in order to give the full optical access for PIV measurement.

1.4 Previous Studies

A number of previous studies have been conducted on hydro power generator.

Carew and Freeston [3] studied the air-flow behaviour in a generator when the air changes direction from circumferential to radial. They built two simple models, an air based model to study the pressure and a water based model to study visually how the flow behaves inside the stator channels. They also studied different stator channel inlet mouth.

According to Lidell et al.[4] a simple and inexpensive modification to solve the over-heating problem is to modify the rotor fan blade. Liddell et al.[4] used CFD calculation and redesigned the existing fan blade in Roxburgh's hydro power generator to increase the mass flow. The results show that the redesigned blades gave 40% pressure increase, a reduction in local viscous losses of 40-60%, but a 10% increase in local windage losses compared to the original blades.

Fujita et al.[5] studied multiple-pitched ventilation ducts to minimize the amount of coolant air in order to minimize windage loss. There are some drawbacks with

their approach. Coil losses and strand loss increase due to non-uniformity of duct distribution.

Moradnia et al.[2] measured the inlet and outlet velocity of the existing generator model at Uppsala University. They studied the generator in cold conditions, which means without heat transfer. The experimental data were then compared to the numerical data that they had done before. The comparisons showed a good agreement between the experiments and the numerical simulations. They suggest that the differences between numerical and experimental results are due to geometrical dissimilarities.

From the previous studies it is apparent that a good ventilation and sufficient air flow in air-cooled generators is very important. The generator temperature should be kept within a design interval to assure the best working conditions and the highest output efficiency.

1.5 Limitations

The present work is limited to one rotor design and two stator designs, straight stator baffle configuration and curved stator baffle configuration. Three different rotor fan blade lengths are studied with each stator design. The Reynolds number is constant and same at Uppsala generator rig [2]. The mass flow and the flow angle has been estimated by using indirect methods.

2 The Experimental Rig

The experimental rig is designed as a 1:2 simplified model of the generator in Uppsala. In the following sections, the experimental rig will be described starting with a general overview, followed by a description of the rotor, the stator, the enclosure, the shaft and the structure. Details of the CAD are attached in the appendix.

2.1 General Overview

Figure 2.1 shows illustrations of the rig. The rig is built solely for the experimental fluid dynamics purposes. The ergonomics of the experimental rig was also taken into account to ensure comfort aspect when doing the experiment. There is no direct relation between comfort and accuracy of the experiment, but we assumed that comfort environment can promote better accuracy.

The overall dimension of the rig is $1\text{ m} \times 0.8\text{ m} \times 1.3\text{ m}$. The height was decided not to be higher than 1.5 m so that it is a convenient height for an average person to set up the experimental devices at the rig. The width, 0.8 m, and length, 1 m, are designed so that it is convenient if the rig has to be moved to another laboratory room. A small width also means that there will be enough space for attaching extra devices without making it difficult to move around the rig.

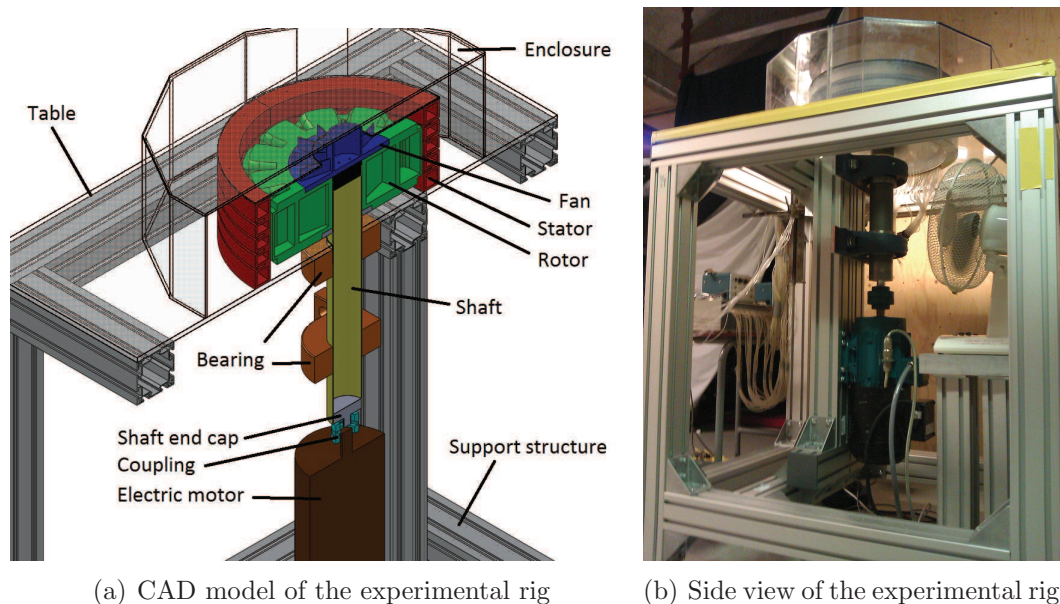


Figure 2.1: The experimental rig

The stator and rotor is placed at the top end of the shaft so that there is no restriction around the interesting region, which is all inside the enclosure. The top

region of the rig is designed to be free from obstacles. There should be no restriction for camera, laser, and other PIV devices that want to access the interesting region of the generator.

2.2 The Rotor

Figure 2.2 shows the rotor geometry which is based on the shape of the rotor of the generator rig in Uppsala[2] but it is simplified for easier CFD mesh generation[6].

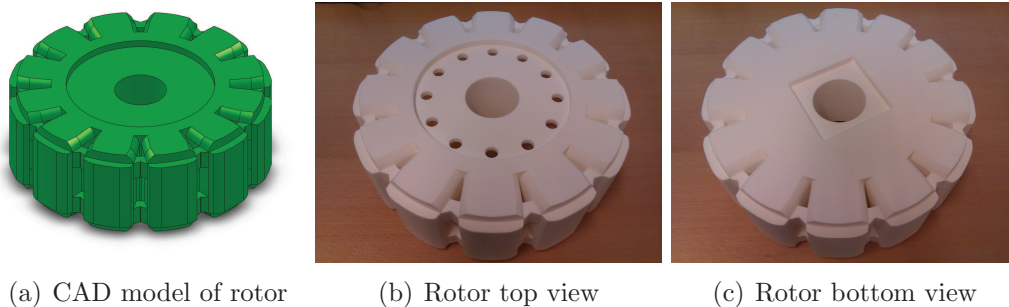


Figure 2.2: The rotor

The rotor has 12 poles. The outer diameter of the rotor is 356 mm and the height of the rotor is 124.80 mm. It has a hollow profile inside to reduce the weight of the rotor. The rotor is made with SLS, Stereo Laser Sintering. This method is also chosen due to the shape complexity of the rotor. SLS produce more ductile structure compare to SLA, Stereolithography Aparatus, thus it can withstand greater forces That is why SLS was chosen for the rotor.

2.3 The Stator

The stator has been built with SLA, Stereolithography Aparatus. This manufacturing process is chosen because SLA can manufacture complex geometries with good accuracy. SLA also gives a smoother surface compare to SLS. This is important since the stator cooling channel in this work is required to be smooth.

Figure 2.3 shows the stator which consists of four parts. A section of stator is made from fully transparent material so that laser light can go through and light the region between the rotor and stator. It is not used in this master thesis project, but this part is an important part for the next study. The stator was divided into four parts due to manufacturing reasons. The final construction is assembled with pieces of plexi-glass and some pieces of rapid-prototyping. The stator has a hollow profile in order to reduce the total weight of the stator, and also there is no necessity for the stator to be solid all around. Lighter stator is easy

to mount and dismount. The outer diameter of the stator is 438 mm, the inner diameter is 365 mm, and the height is 174.80 mm.

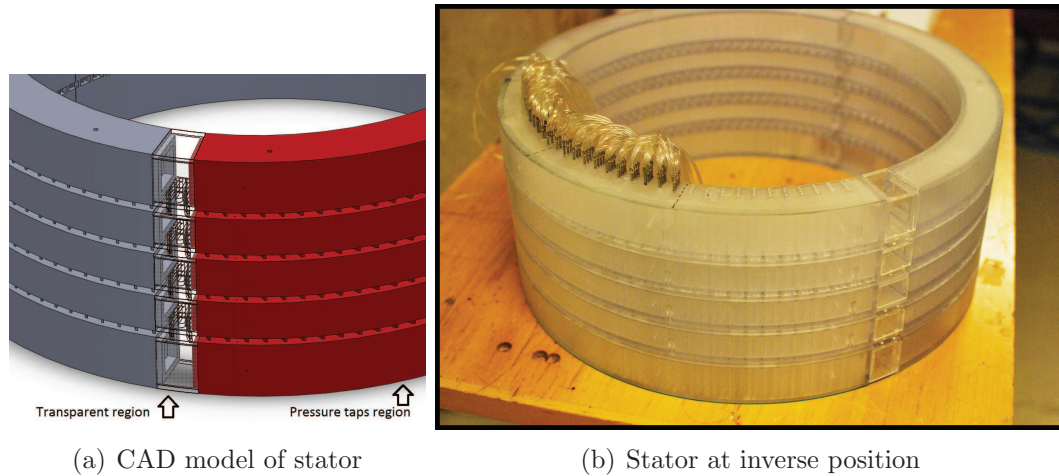


Figure 2.3: The stator

Two stator layouts have been studied in this work. The first stator has straight channels and the second stator has curved channels, as shown in figure 2.4. The straight baffles of stator cooling channel has a benefit in terms of optical access compared to the curved baffles. Figure 2.4 shows the two stator layouts.

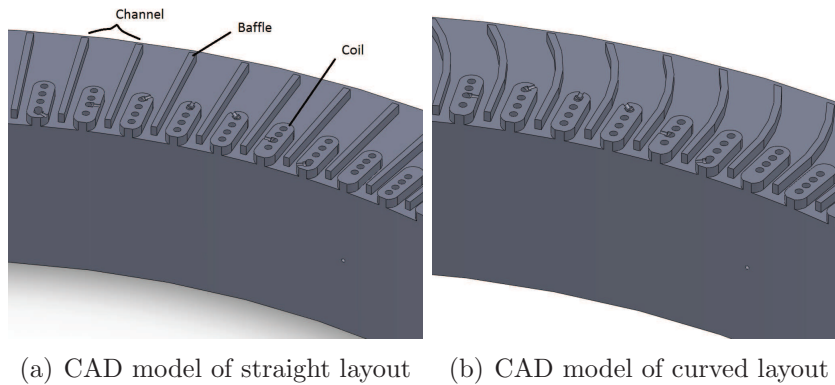


Figure 2.4: CAD model of the stator cooling channel layout

2.4 The Fan Blades

Fan blades are added to increase the air mass flow into the generator cooling channel. The fan blades are attached on top of the rotor, see figure 2.5. The fan used in this project has 12 straight radial blades with three different lengths;

short, 42.50 mm; medium, 85 mm; long, 99.50 mm starting at the shaft radius. The height of the fan blades is 25 mm and the thickness is 1.5 mm. The fan is made with the same manufacturing process as the rotor (SLS).

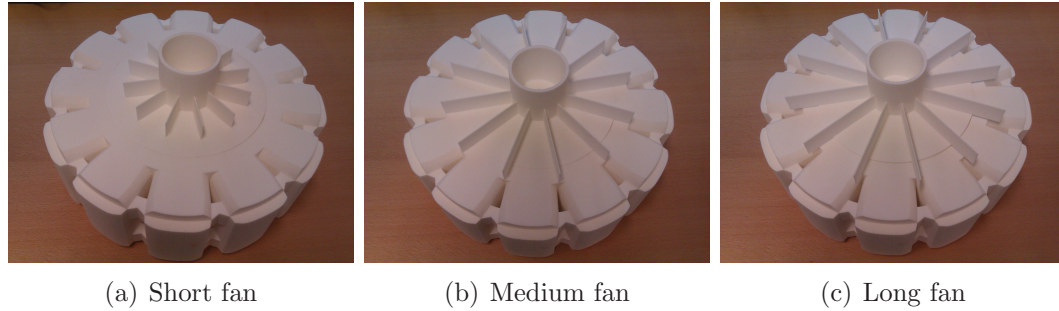


Figure 2.5: The fan blade

2.5 The Top Lid

Top lid is added to define the inlet boundary. The top lid in present work is a 3 mm thick transparent plexi-glass cover disk with same diameter as stator. It has a 120 mm diameter opening at the center, which will serve as the air inlet. This top lid is attached on the top of the stator, as seen at figure 2.6.

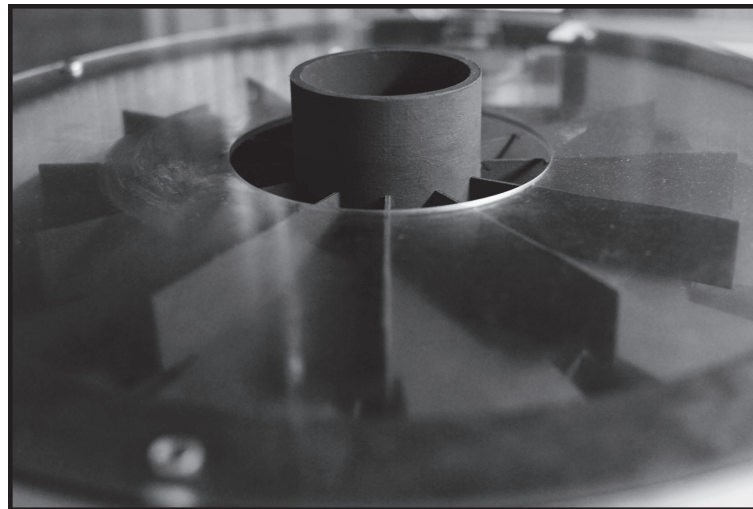


Figure 2.6: The top lid

The combination between enclosure and top lid creates a defined inlet condition. First the air will go radially into the axis center and then it will be forced to turn axially to enter the lid and then it will go radially again towards the channel.

2.6 The Enclosure

The term enclosure in this context refers to a large transparent cover which together with the acrylic table closes the generator outer boundaries, see figure 2.1. With this enclosure, the rig is a closed loop system, which means that the air inside the enclosure will recirculate.

Figure 2.7 shows the different components of the enclosure. The enclosure has a polygonal shape with 12 tangential sides. The inner diameter is 657 mm and the height is 215 mm. The enclosure was manufactured in three parts; the top part and two side walls. The three parts are glued together into one. The material used is polycarbonate with 5 mm thickness.

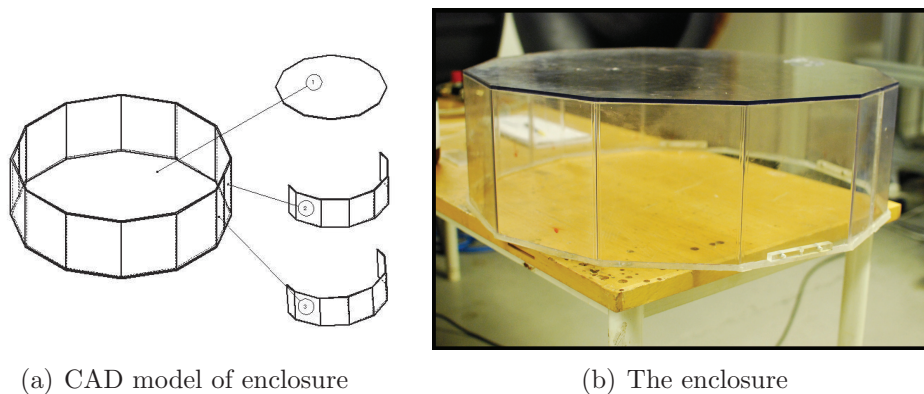
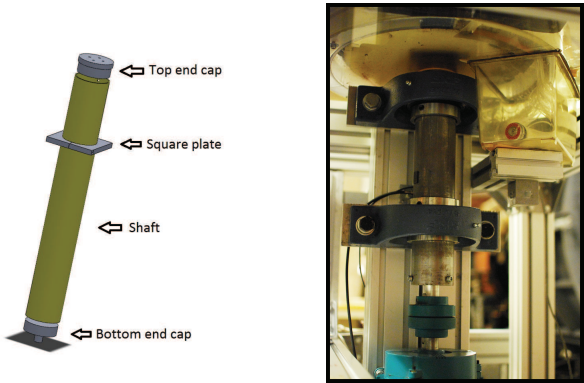


Figure 2.7: The enclosure

The polygonal shape of the enclosure is chosen due to manufacturing limitations. Also, for laser measurement, it is better to have flat surfaces rather than circular ones, as a flat surface creates less distortion.

2.7 The Shaft

The rig has a 500 mm hollow stainless steel shaft with 3 mm thickness and 70 mm outer diameter, as shown in figure 2.8. A hollow shaft is lighter, better in terms of stiffness to mass ratio, and has a higher natural frequency which is desired for rotating machinery. Attached to the shaft, there is a square plate to prevent the rotor from rotating relative to the shaft and from falling down. The top and bottom end caps are made from aluminium.



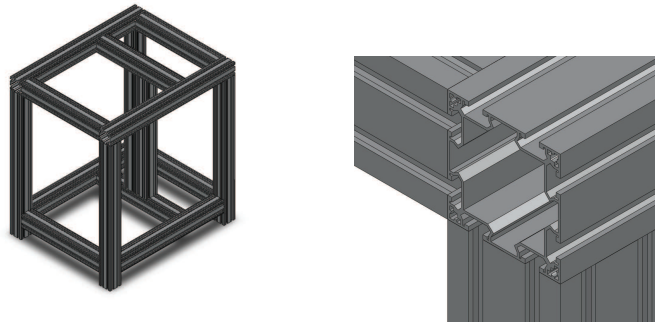
(a) CAD model of shaft with its components (b) Shaft and its component in the rig

Figure 2.8: The shaft

The shaft is held by two bearings. The bearings that is used are two pillow block units SKF bearing (SYJ-70-TF). Those bearings are used to support the rotor to stiffen the shaft and also to prevent misalignment and minimize vibration.

2.8 The Experimental Rig Support Structure

The support structure is made from aluminium profiles, as shown in figure 2.9. This kind of aluminium profile is chosen because of its flexibility in terms of assembling. It has numerous available accessories that are available and easy to attach. With these profile adding new features to the rig is simple and can be done in a short time.



(a) Overview of the rig support structure (b) The shape of the aluminium profile

Figure 2.9: The experimental rig support structure

3 Methodology

In this following section, the methodologies are described for the static pressure measurement, the total pressure measurements and the mass flow estimation.

3.1 Static Pressure Measurement

For the static pressure measurements the stator is instrumented with pressure taps at the walls. According to Anthoine et al. [7], the best hole diameter of a pressure tap should be approximately 0.5 mm. For diameters smaller than 0.5 mm the time response is longer and the hole may easily get blocked by dust. For diameters larger than 0.5 mm, the pressure taps can introduce distortion to the flow fields which makes the measurement less accurate. The best measurements are obtained with small, sharp edged holes that are perpendicular to the wall.

Figure 3.1 shows the axial arrangement of the static pressure channels through the stator body. The pressure taps have an expansion from 0.5 mm to 1.4 mm as seen in figure 3.1(b). The pipes go through the stator coils so that they do not disturb the fluid flow. All pressure pipes exit at the bottom of the stator body, to make the connection to the pressure transducer easier and not to disturb the flow. The coil in each stator cooling channel has only one pressure tap and in one particular position. This is due to the space limitation, and in order to follow the requirements of a good pressure tap.

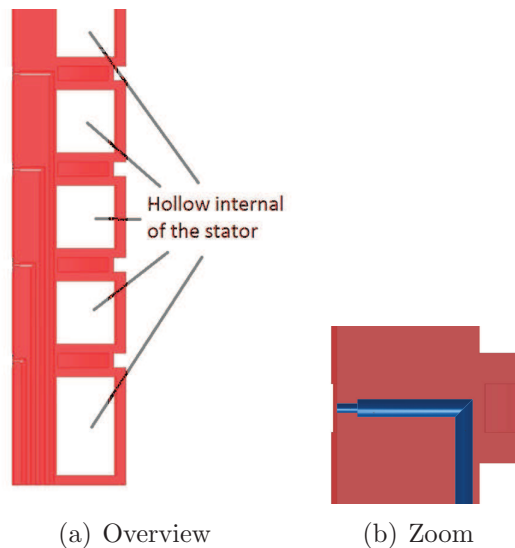
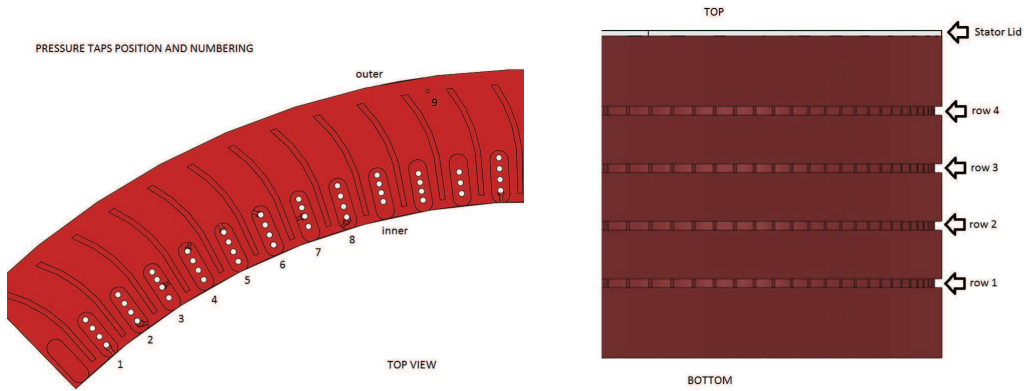
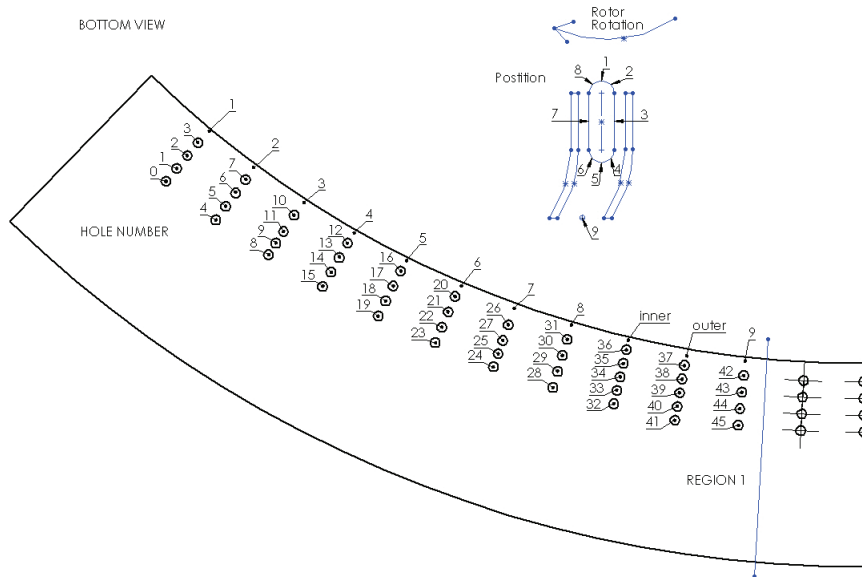


Figure 3.1: Illustration of the pressure pipe



(a) Position numbering

(b) Row numbering



(c) Hole Numbering

Figure 3.2: The Map of Static Pressure Holes

There are a total of 138 pressure taps in the stator, in fact only 92 pressure taps were used and the rest were kept for substitution if there was a malfunction of any of the pressure taps.

A special map is created in order to distinguish which pressure channels belong to which holes. In this project the map is as seen in figure 3.2. The map in figure 3.2 just shows one third of the total hole. This is because the other two thirds have

the same pattern. There are numbering for position of the pressure taps around the coils and at the channel outlet (position 1-9), numbering for the exit holes (hole number 0-45) and numbering for row (row 1-4). For row numbering, row number 1 is the bottom most and row number 4 is the top most. The map is designed so that the data set always from the top most row to the bottom most row for each position of the pressure taps.

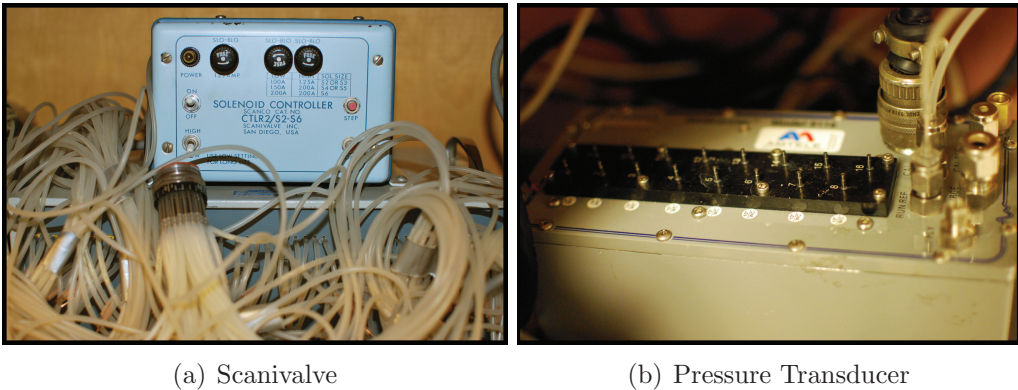


Figure 3.3: Pressure measurement devices

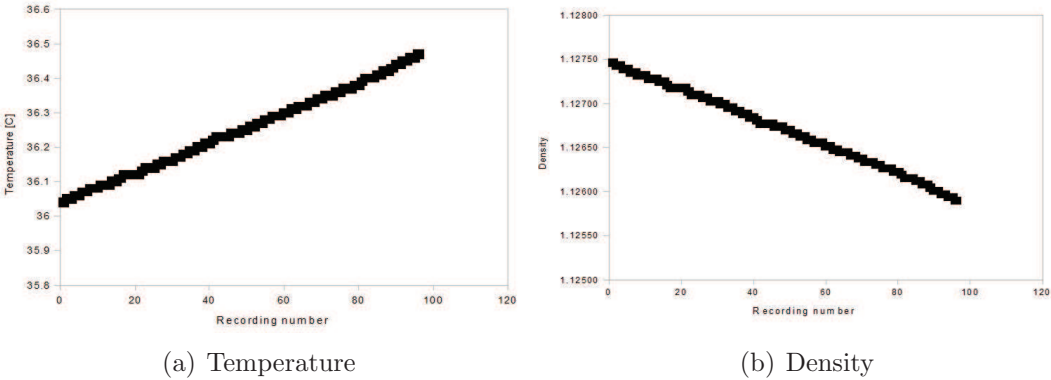


Figure 3.4: Sample of temperature and density stability from short fan blade and straight stator baffle configuration

The pressure is recorded with pressure transducer device and two scanivalve devices, as seen in figure 3.3. The advantage of using scanivalve is if the quantity of pressure taps are more than the capacity of the pressure transducer. The scanivalve will separate the reading of all pressure taps by reading only one pressure taps each time. The drawback of this method is that the pressure is not recorded at the same instance in time for all pressure taps.

As long as the temperature has stabilized, the mean pressure is unaffected by this drawback. One example of temperature and density stability from a typical experimental run is seen in figure 3.4.

Figure 3.4 shows an example of the temperature and density developments during a measurement. The change of air density is less than 2%, which is considered small enough not to significantly affect the results.

The sampling rate is 500 samples per second and the samples have been averaged over time. The measurement time is 2 seconds for each pressure tap, corresponding to 800 rotor pole passes.

3.2 Total Pressure Measurement

The pressure rake used in this project is custom made for the rig and is shown in figure 3.5. It is comprised of 14 pipes, each made up of three steel pipes of different diameter and length. The tip of each pipe is 0.5 mm in diameter with 40 mm length. This tip is then connected to a 0.8 mm diameter pipe with 333 mm length. At the very end, each pipe is connected to another 1.4 mm diameter pipe with 15 mm length. All the 14 pipes are put side by side and glued together with epoxy glue.

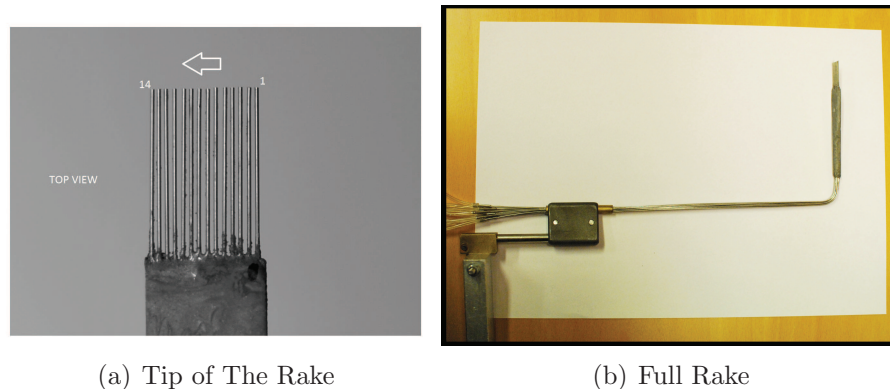


Figure 3.5: The Rake

The function of this rake is to measure total pressure at the outlet of the channel. By measuring the total pressure at the outlet, the performance of the channel can be estimated. Figure 3.6 shows the illustration of how the measurement has been done.

The rake is located at the middle of the channel height and located exactly at the end wall of the baffles. The rake angle follows the curvature of the baffles. For the straight stator design it is radial, and for the curved stator design follows the exit curvature of the baffles. 11 pipes were in between two baffles and 3 pipes were

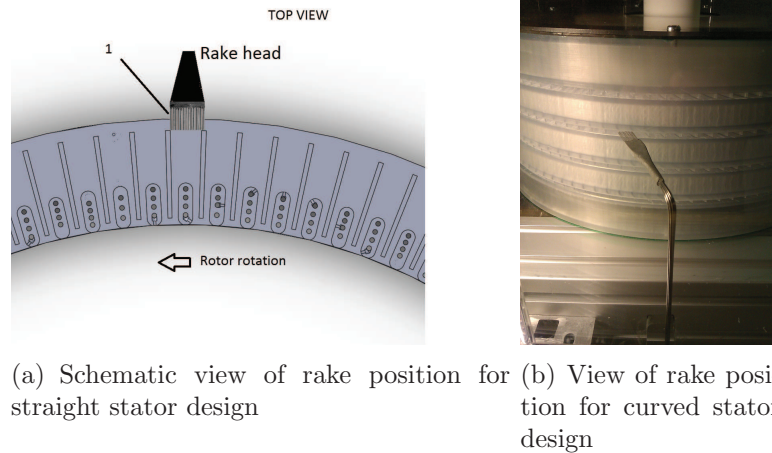


Figure 3.6: Rake position in the measurement

outside the channel due to the width of the rake is larger than the width of the stator channel.

The rake measurements have been done by connecting directly all the pipes to the 16 channel pressure system. The pressures are thus simultaneously read. The sample rate is 500 sample per second with a duration of 2 seconds, corresponding to 800 rotor pole passes. The samples are then averaged in time.

3.3 Mass Flow Estimation

Cooling air mass flow is an important feature in air cooled generator. According to Hudon et al. [8], there should be a balance between fluid flow rate and ventilation losses. Too much air coming into the generator will increase the ventilation losses and will lower the global efficiency of the generator itself. On the other hand, low fluid flow rate will rise the temperature and life expectancy will be reduced.

Mass flow is estimated from total pressure reading at the channel outlet. The flow inside the channel is assumed to be fully developed with a very thin boundary layer at the top and bottom channel walls. Flow is assumed to be symmetric and do not have large velocity gradient. The outlet velocity can be estimated from dynamic pressure equation. The static pressure at the stator cooling channel is assumed to be constant so that when total pressure is subtracted with static pressure at the stator cooling channel outlet, the result is dynamic pressure. By rearranging the equation for dynamic pressure the velocity can be obtained. And mass flow in one channel is obtained via an integration of the velocity distribution across outlet channel area. For all channel row, multiply the value with total number of stator cooling channels in the row. And for total estimated mass flow, add together the mass flow from each row.

$$\begin{aligned}
p_{dynamic} &= 0.5\rho V^2 \\
V^2 &= 2p_{dynamic}/\rho \\
V &= \sqrt{2p_{dynamic}/\rho}
\end{aligned}
\tag{3.1}$$

$$\dot{m} = \sum V \Delta x t \rho
\tag{3.2}$$

3.3.1 Flow Angle Estimation From Static Pressure Measurement at The Enclosure

Static pressure reading between two points (P1 and P2) located at the enclosure, as shown in figure 3.7 can be used to estimate the flow angle.

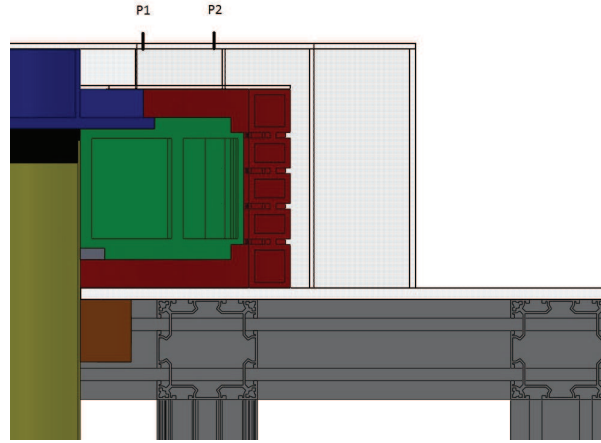


Figure 3.7: Illustration of Pressure Tap Location at the Enclosure

Continuity equation, conservation of rotation and Bernoulli's equation are used to calculate the absolute inlet velocity. Some assumption has been made in order these equations are valid. The flow at inlet is assumed to be incompressible, inviscid and steady. The pressure gradient along the inlet height is also assumed to be zero.

For radial component of the flow the continuity equation will be as follows,

$$\begin{aligned}
\rho v A &= constant \\
\rho v_1 A_1 &= \rho v_2 A_2 \\
\rho v_1 (2\pi r_1 h) &= \rho v_2 (2\pi r_2 h) \\
v_2 &= v_1 \frac{r_1}{r_2}
\end{aligned}
\tag{3.3}$$

For tangential component, the conservation of rotation equation is used,

$$\begin{aligned}
 wr &= \text{constant} \\
 w_1 r_1 &= w_2 r_2 \\
 w_2 &= w_1 \frac{r_1}{r_2}
 \end{aligned} \tag{3.4}$$

The flow angle, α , is defined as,

$$\tan \alpha = \frac{w}{v} \tag{3.5}$$

Input the continuity and conservation of rotation equation into the Bernoulli's equation

$$\begin{aligned}
 p + 0.5\rho V^2 &= \text{constant} \\
 p_1 + 0.5\rho V_1^2 &= p_2 + 0.5\rho V_2^2 \\
 p_2 - p_1 &= 0.5\rho V_1^2 - 0.5\rho V_2^2 \\
 \Delta p &= 0.5\rho (V_1^2 - V_2^2) \\
 \Delta p &= 0.5\rho ((v_1^2 + w_1^2) - (v_2^2 + w_2^2)) \\
 \Delta p &= 0.5\rho ((v_1^2 + v_1^2 \tan^2 \alpha) - (v_2^2 + v_2^2 \tan^2 \alpha)) \\
 \Delta p &= 0.5\rho \left((v_1^2 + v_1^2 \tan^2 \alpha) - \left(v_1^2 \left(\frac{r_1}{r_2} \right)^2 + v_1^2 \left(\frac{r_1}{r_2} \right)^2 \tan^2 \alpha \right) \right) \\
 \Delta p &= 0.5\rho v_1^2 \frac{1}{\cos^2 \alpha} \left(1 - \left(\frac{r_1}{r_2} \right)^2 \right) \\
 \cos^2 \alpha &= 0.5\rho v_1^2 \frac{1}{\Delta p} \left(1 - \left(\frac{r_1}{r_2} \right)^2 \right) \\
 \alpha &= \cos^{-1} \left(0.5\rho v_1^2 \frac{1}{\Delta p} \left(1 - \left(\frac{r_1}{r_2} \right)^2 \right) \right)^{0.5}
 \end{aligned} \tag{3.6}$$

All variables which are needed to estimate the flow angle have been measured. The pressure difference has been measured, the radius of pressure taps location at the enclosure has been known and the estimated mass flow has been obtained in previous chapter. The radial direction velocity at the inlet then can be calculated from the local mass flow equation as follows

$$\begin{aligned}
 \dot{m} &= \rho v_1 2\pi r_1 h \\
 v_1 &= \dot{m} / (\rho 2\pi r_1 h)
 \end{aligned} \tag{3.7}$$

By inserting all the variables into equation 3.6, the estimated flow angle can be obtained.

3.4 Error Estimation

There are two types of error, random error and bias error, according to Anthoine et al.[7]. The random error is happened e.g. when same person and same device performed repeated trials of an experiment. Random error can be calculated from ratio of standard deviation of the data around the mean and square root of number of taken samples.

$$error_{statistical} = std/\sqrt{N} \quad (3.8)$$

The bias error is usually fixed and is determined by engineering judgement. The bias error can be an error of the measurement device itself. In present work, the bias error is $\pm 0.2 Pa$.

Total error can be estimated as,

$$error_{total} = \sqrt{error_{statistical}^2 + error_{measurement}^2} \quad (3.9)$$

4 Results and Discussion of the Pressure Measurement

In this chapter, the results from the measurements will be discussed. The measurements were done point by point. The linear interpolated lines are added for better visualisation. Raw data from each configuration has been plotted in figure A.1.

4.1 Static Pressure Measurements Around The Stator Coils and Outlet of the Stator Channel

The air flow inside the channel has been investigated by measuring the static pressure distribution around the coils and at the outlet of the channels.

In figure 4.1 the static pressure is separated for every row so that it is easier to analyse the pressure variation inside the different rows in the generator. Diamond, triangle, hexagram, and star represent static pressures at row number 1, 2, 3, 4 respectively.

The flow enters the stator cooling channels in an angle, which is noticed by highest static pressure at pressure tap position 2, i.e. pressure tap at position 2 is a stagnation point. From case to case static pressure around the coil except at the stagnation point does not differ much. In most cases the stagnation pressure highest at row 1 or 2. For configuration with medium fan blade and curved stator, the stagnation pressure values in row 1,3,4 are close to each other, we can say that the pressure distribution in this configuration is more uniform compare to other configurations.

4.2 Static Pressure Measurements at Stator Walls, Inner and Outer

A total of 20 pressure taps were used to measure static pressure at inner and outer stator walls. 5 pressure taps at inner wall and 5 at outside in 2 repetitions.

Figure 4.2 shows that the static pressure is higher in lower row. The static pressure is higher at inner stator wall compare to outer stator wall. This is true, since flow is moved from higher pressure to lower pressure region. There is an increment of static pressure difference between the inner and outer wall. It is not so obvious in curved stator layout but it is clearly seen in straight stator layout. The longer the fan blade the higher the pressure difference. We can relate this pressure with losses so we can estimate the losses of each configuration. The bigger the pressure differences the bigger the losses.

4.3 Total Pressure Measurement at The Outlet of Stator Cooling Channel with Total Pressure Rake

The total pressure distribution at the outlet of the stator cooling channels has been measured with a total pressure rake. Figure 4.3 shows the comparison between all the configurations. The graphs only show 11 measurement points due to the size reason between the rake and the stator outlet channel. The static pressure at the outlet channel (position 9 at figure 4.1) is used as the reference pressure.

Zero or negative reading in Figure 4.3 means that the velocity is nearly zero with respect to the total pressure probe direction, i.e. there is a recirculation region. It can be concluded that half of the channel is occupied by the recirculating flow, and just half of the channel is effective in transferring the air.

4.4 Mass Flow Estimation from Total Pressure Measurement at The Stator Cooling Channel

The mass flow estimations from the total pressure rake measurements are shown in table 4.1. For curved channel, the longer the fan blade the higher the mass flow. The difference between the straight and curved stator design is not large except for the case with the longest fan blade.

Table 4.1: Mass flow estimation from total pressure measurement at the stator cooling channel

Mass flow [kg/s]		blade
straight stator	curved stator	
0.1028	0.0939	short
0.1206	0.1236	medium
0.1077	0.1291	long

4.5 Flow Angle Estimation From Static Pressure Measurement at the Enclosure

Results of the flow angle estimation are shown in table 4.2. Flow angle for curved stator seems constant in approximately 70° angle. Another feature that we can see from table 4.2 is, the longer the fan blade the smaller the flow angle. This big angle is due to curved stator cooling channel redirect the flow in an angle at its outlet.

More complex behaviour is observed for straight configuration. The flow angle is smallest for the medium fan (near 20°) and rather large (60°). For sure the outlet

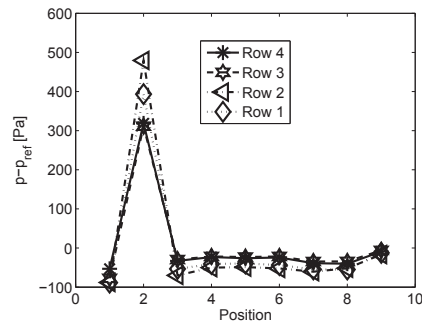
air from stator cooling outlet is straight. The shaft and fan rotation at the top is suspected for introducing the swirl into the whole domain. The rotation causes the air flow to swirl.

Table 4.2: Flow angle estimation from static pressure measurement at the enclosure

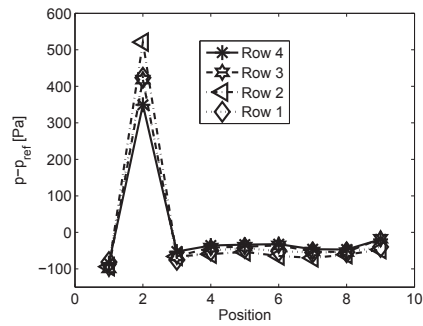
Flow angle		blade
straight stator	curved stator	
58.97°	69.54°	short
22.95°	66.78°	medium
36.69°	66.18°	long

4.6 Error Estimation

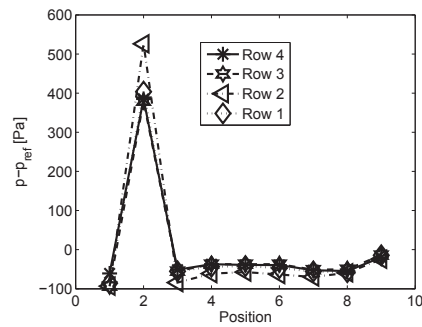
Error of pressure measurement in this project is approximately 0.22 Pa. This can be considered small, because it almost the same as the error in the measurement devices itself (bias error, i.e 0.2 Pa). The value is calculated from 500 samples and 2 seconds measurement, i.e. 1000 samples.



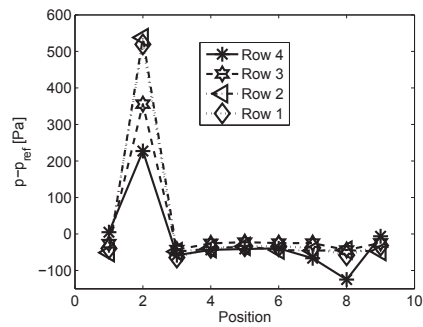
(a) Short fan blade, curved stator channel



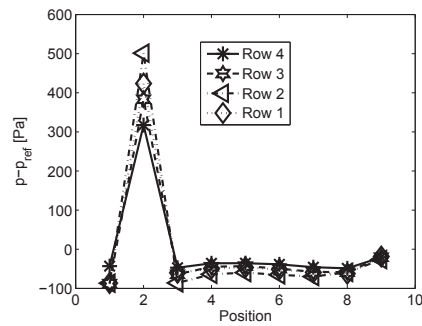
(b) short fan blade, straight stator channel



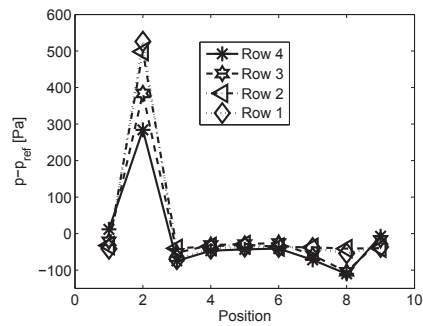
(c) Medium fan blade, curved stator channel



(d) Medium fan blade, straight stator channel

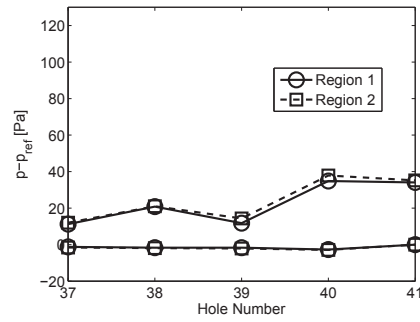


(e) Long fan blade, curved stator channel

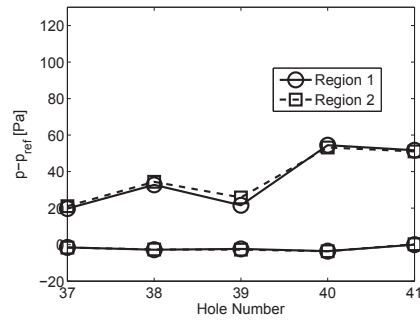


(f) Long fan blade, straight stator channel

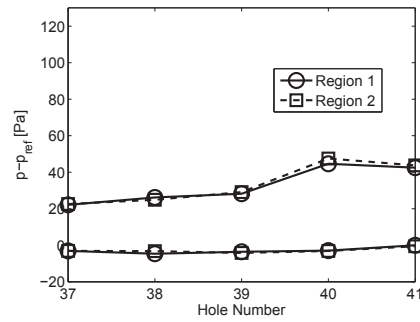
Figure 4.1: Static pressure distribution around the coil



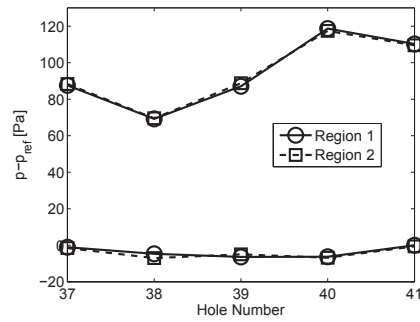
(a) Short fan blade, curved stator channel



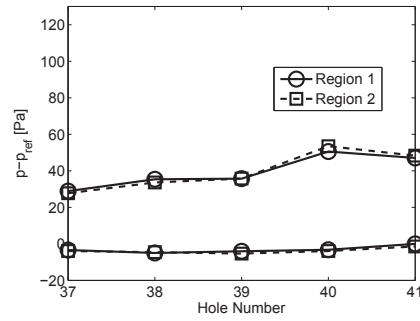
(b) Short fan blade, straight stator channel



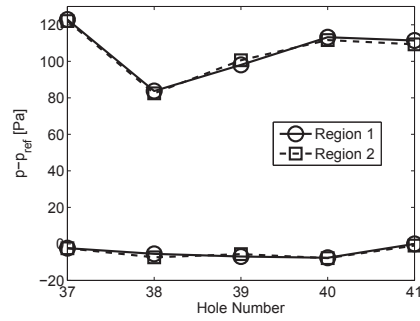
(c) Medium fan blade, curved stator channel



(d) Medium fan blade, straight stator channel

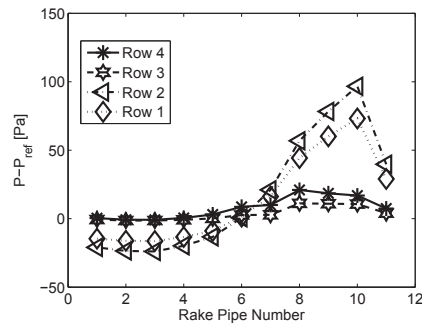


(e) Long fan blade, curved stator channel

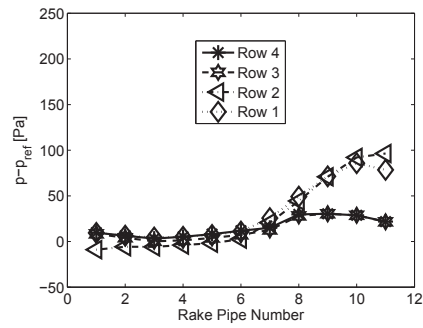


(f) Long fan blade, straight stator channel

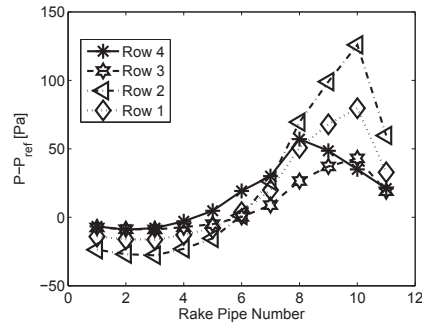
Figure 4.2: Static pressure on the inside and outside stator walls



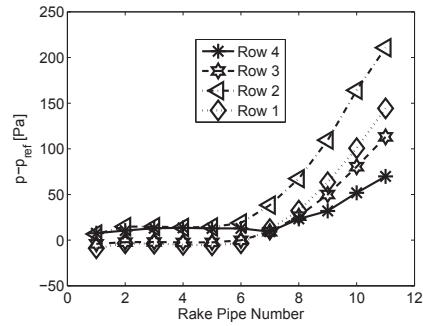
(a) short fan blade; curved stator channel



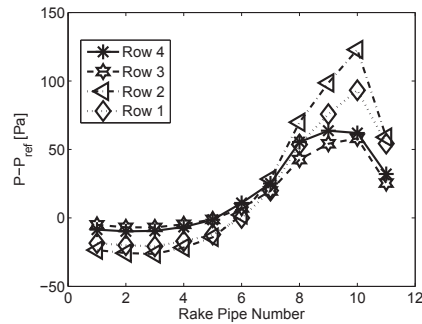
(b) short fan blade; straight stator channel



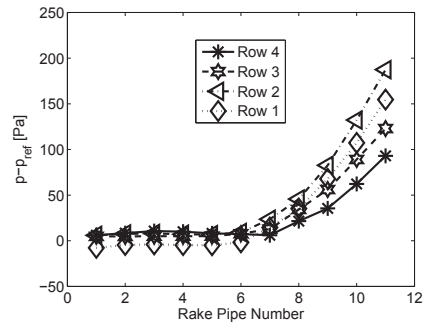
(c) medium fan blade; curved stator channel



(d) medium fan blade; straight stator channel



(e) long fan blade; curved stator channel



(f) long fan blade; straight stator channel

Figure 4.3: Relative total pressure distribution at the channel outlet. A zero or negative value corresponds to a recirculation region

5 Conclusions

This work presents the design and construction of an experimental rig for studying air flow in a generator model. Evaluation of rig performance with 2 different stators and 3 fan configurations and results of measurements of static and total pressure are also presented.

The rig has been designed for experimental fluid mechanics purposes. Pressure taps have been embedded in the stator body not to disturb the fluid flow. A transparent region for PIV measurement has been prepared, such as, table, some of the stator walls, some stator cooling channels, lid and the enclosure. Some simplifications have been made to meet the requirements of future numerical simulations.

The rapid prototyping methodology, based on SLA and SLS, was used to manufacture most of the generator model. Rapid prototyping achieves high detailization and complexity of the generator model with good accuracy. Ordinary manufacturing processes are difficult due to the size of the model and the geometry complexity.

The stagnation pressure at the stator coil increases as the air flows axially inside the stator. Static pressure around the coils shows that the air does not enter the channel radially, but with an angle. This cause the stagnation point to shift off from the center of the coils. It also causes flow separation and a recirculation behind the coils. Total pressure measurements with rake at the stator channel outlet show that half of the stator cooling channel is occupied with the recirculation region.

The inlet mass flow is shown to be proportional to the length of the fan blade for the curved stator design, for the straight stator design the maximum mass flow is achieved for medium fan. A higher mass flow also appears with the curved stator channel design, compared to the straight stator channel in all cases.

Highly swirl flow is estimated at curved stator, with approximately 70° flow angle. For the straight stator there is also a swirl effect. We suspect that the rotation of the shaft and fan caused the swirl.

6 Future Work

There is always room for improvement and ideas for future studies. The following notes are provided as advices to consider during future works.

The pressure measurement methodology in the present work is restricted to time-averaged results. Time resolved measurements would be of high interest. With PIV (Particle Image Velocimetry) an estimation of the unsteady behaviour can be made.

The fan blade length has proved to influence the mass flow. This work was restricted to straight fan blades with different lengths. Different kinds of shape and length of the fan blades may be of interest for future studies.

Measuring the torque at the shaft could be a good idea. By knowing the torque, the air resistance can be predicted and also the air resistance due to the geometry of the fan blades or rotor can be studied.

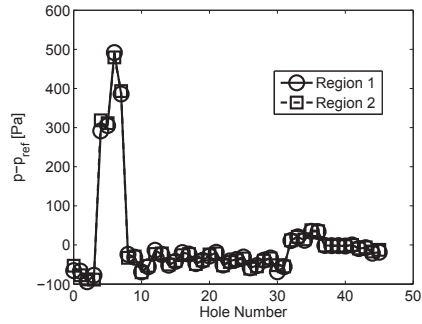
New rotor and stator designs can easily be manufactured using the rapid prototyping technology. An example is the inclusion of bent stator channel baffles for pick-up purposes.

References

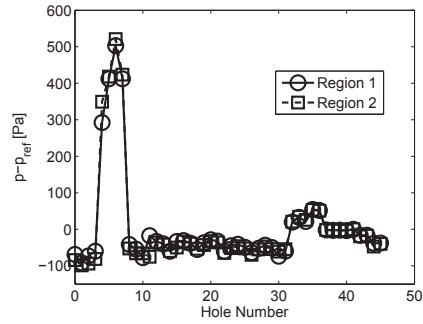
- [1] “Hydro power.” Available at: <http://www.el.angstrom.uu.se/forskningsprojekt/HydroPower.html>, Division For Electricity, Uppsala University, The Ångström Laboratory, Box 534, 751 21 Uppsala, 2 March 2011.
- [2] P. Moradnia, V. Chernoray, and H. Nilsson, “Experimental and numerical investigation of the cooling air flow in an electric generator,” in *8th International Conference on Heat Transfer, Fluid Mechanics and Thermodynamics*, 11-13 July 2011.
- [3] N.J.Carew and D. Freeston, “Fluid Flow Losses in A.C. Generator Stator Ventilating Ducts,” *Proc Instn Mech Engrs*, vol. 182, no. 12, pp. 87–95, 1967-1968.
- [4] B. Liddell, A. Tucker, I. Huntsman, M. Manders, and C.McDonald, “Re-designing the Rotor Fan Blades to Improve the Cooling of Roxburgh’s Hydro-Generators,” in *14th Australian Fluid Mechanics Conference*, (Adelaide University, Adelaide, Australia), pp. 465–468, 10-14 December 2001.
- [5] M. Fujita, Y. Kabata, T. Tokumasu, M. Kakiuchi, H. Shiomi, and S. Nagano, “Air-cooled large turbine generator with multiple-pitched ventilation ducts,” *IEEE*, pp. 910–912, 2005.
- [6] P. Moradnia and H. Nilsson, “CFD of Air Flow In Hydro Power Generator for Convective Cooling, Using OpenFOAM,” in *V European Conference on Computational Fluid Dynamics* (J. Pereira and A. Sequeira, eds.), (Lisbon, Portugal), ECCOMAS CFD 2010, 14-17 June 2010.
- [7] J. Anthonie, T. Arts, H. Boerrigter, J.-M. Buchlin, M. Carbonaro, G. Degrez, R. Denos, D. Fletcher, D. Olivari, M. Riethmuller, and R. V. den Braembussche, *Measurement Techniques in Fluid Dynamics; An Introduction. 3rd revised edition*. The Von Karman Institute, 2009.
- [8] C. Hudon, A. Merkhouf, M. Chaaban, S. Belanger, F. Torriano, J. Leduc, F. Lafleur, J. F. Morissete, C. Millet, and M. Gagne, “Hydro-Generator Multi-Physic Modelling,” vol. X-n^o x/annee, p. 1 a X, 2009.

A Appendix: Periodicity of The Flow

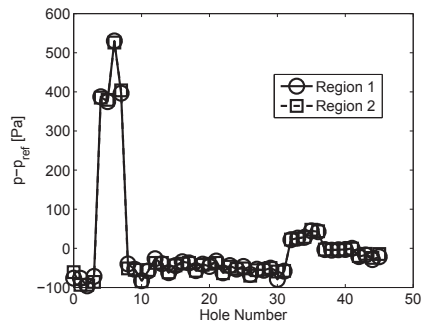
Figure A.1 shows the raw data of the experiment. Post processing has been done and the pressure has been separated for every row in section 4.1 and section 4.2. The map at figure 3.2 helps to separate the pressure data when doing the post processing. By comparing raw data, the periodicity error can be estimated. If the flow 100% periodic, the data in region 1 and 2 will match perfectly. Slight differences means there is a slight non periodicity in the flow. Periodic flow is important due to method that is used to measure static pressure around the coil needs periodic flow. It is because each coil only has one pressure tap in one position. Periodic flow makes this method work, because the pressure in one particular position will be the same at any coil where the pressure is measured.



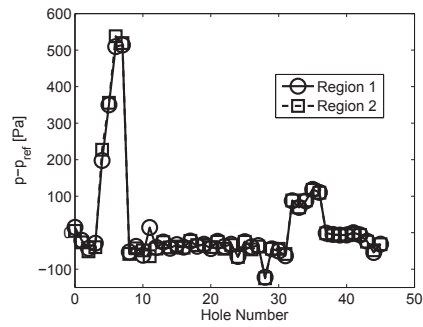
(a) short fan; curve stator layout



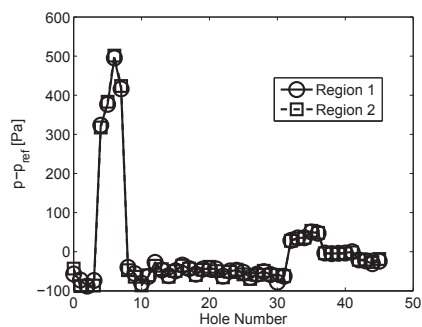
(b) short fan; straight stator layout



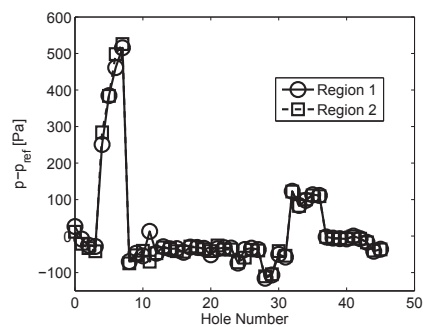
(c) medium fan; curve stator layout



(d) medium fan; straight stator layout



(e) long fan; curve stator layout

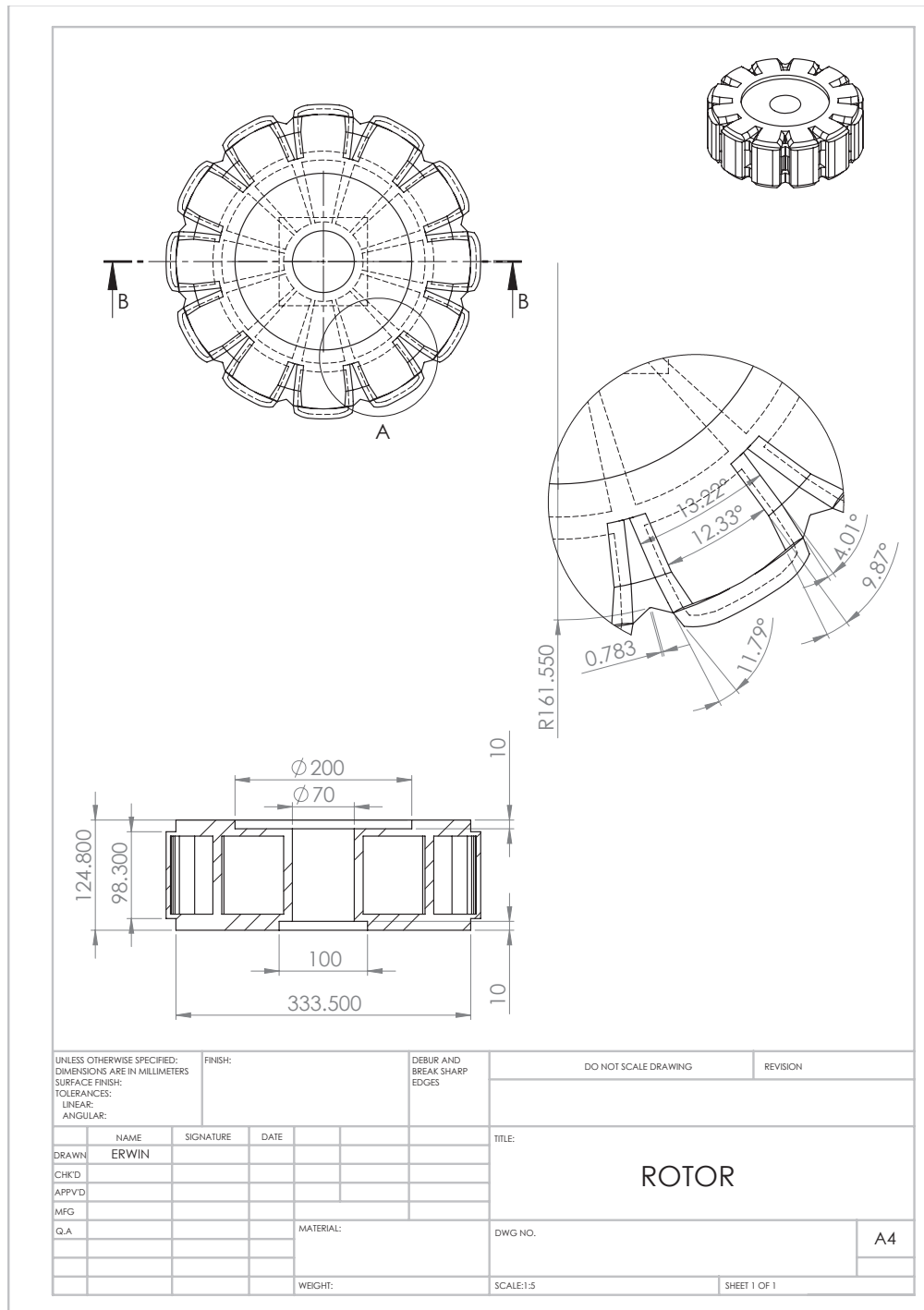


(f) long fan; straight stator layout

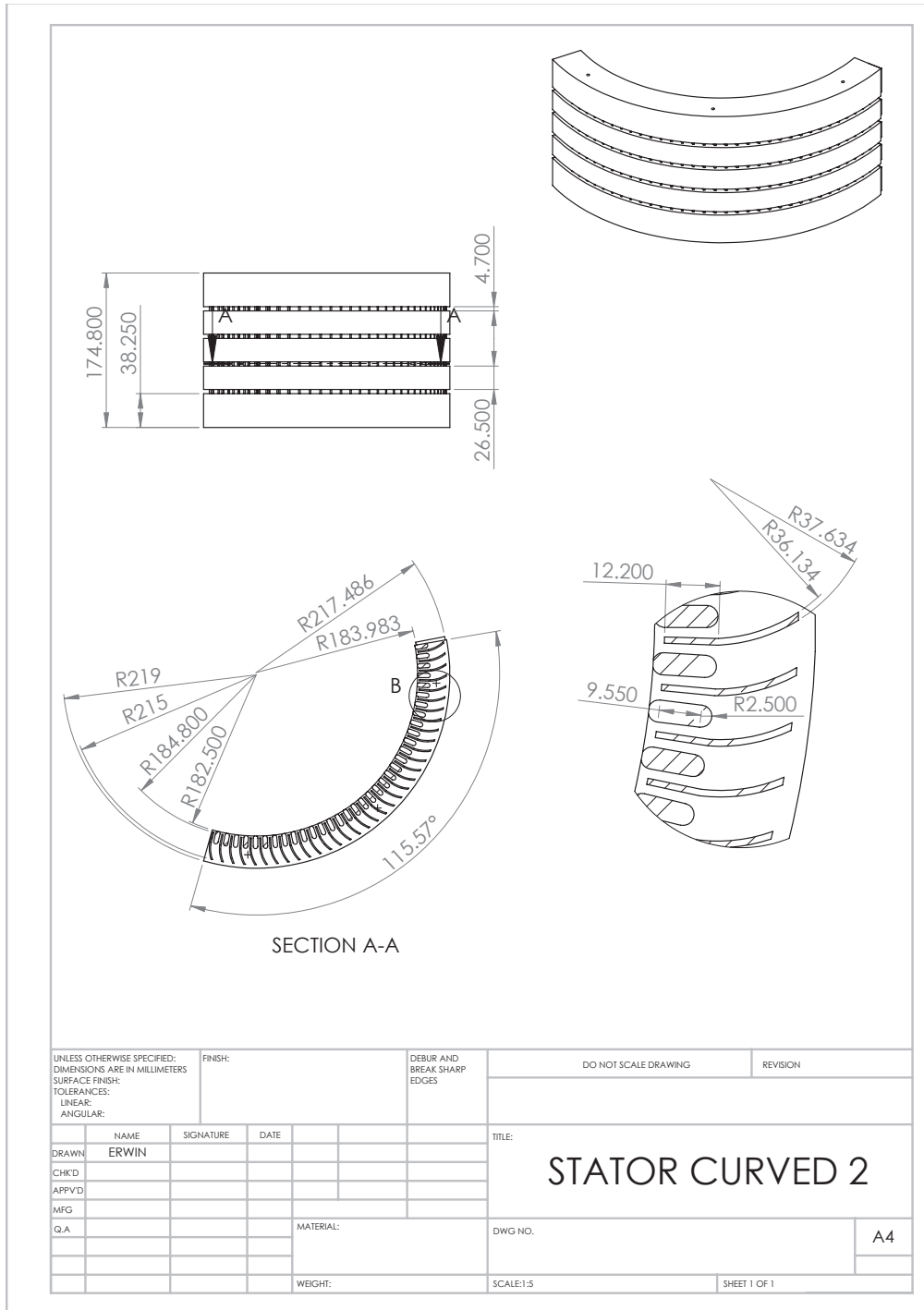
Figure A.1: Static pressure comparison in two stator channel layout

B Appendix: CAD Drawings

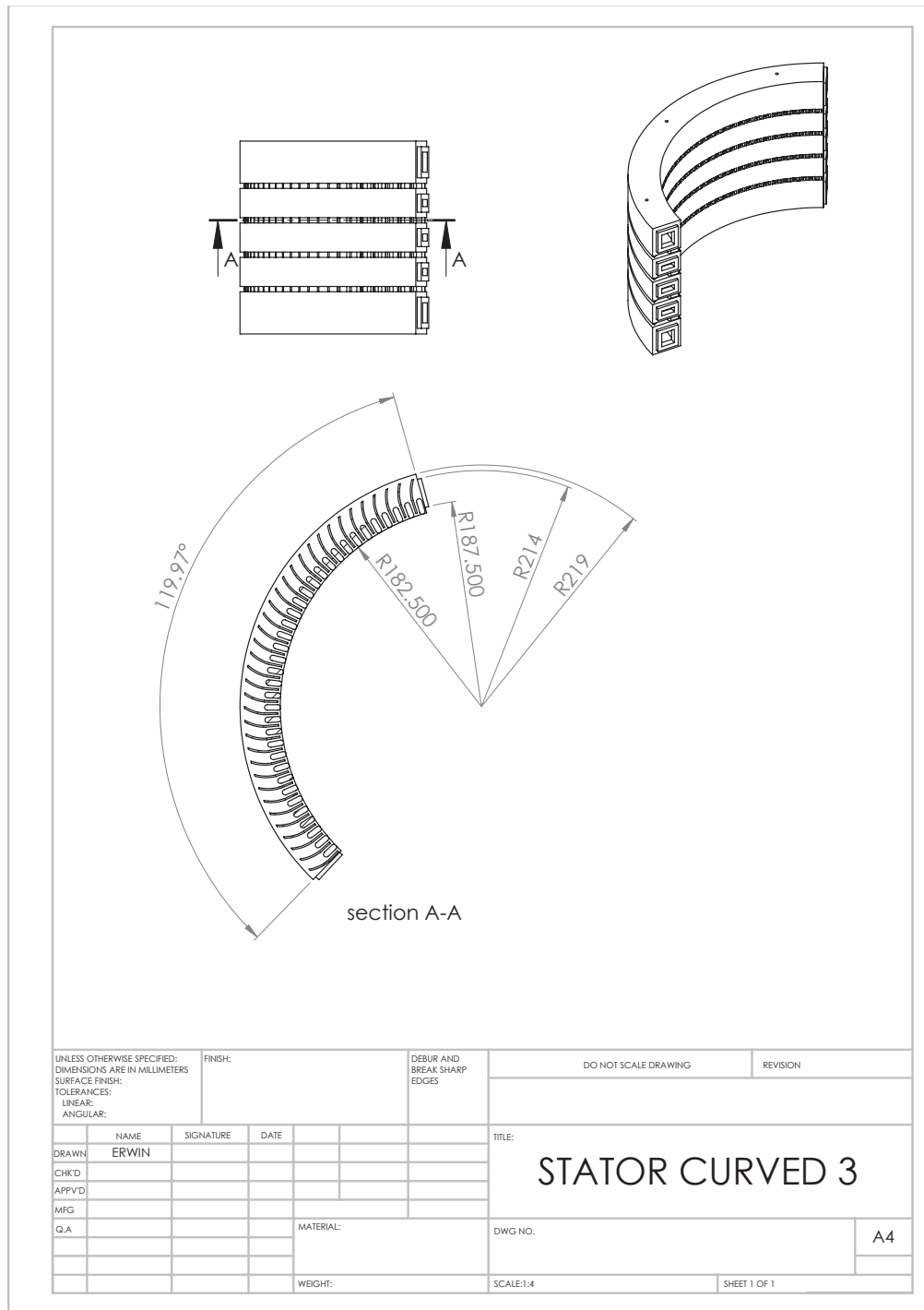
B.1 Rotor



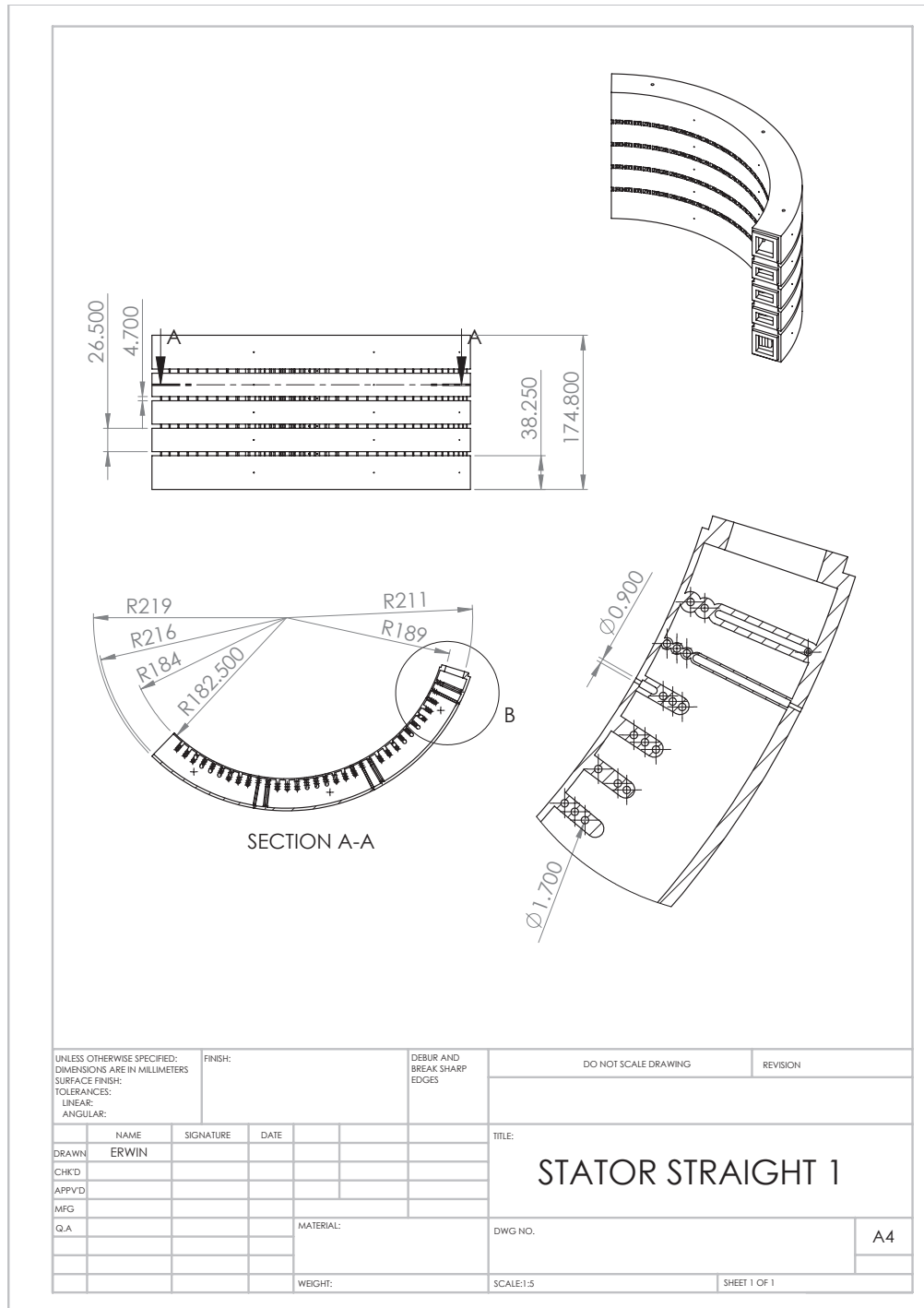
B.3 Stator Curved Baffles 2 of 3



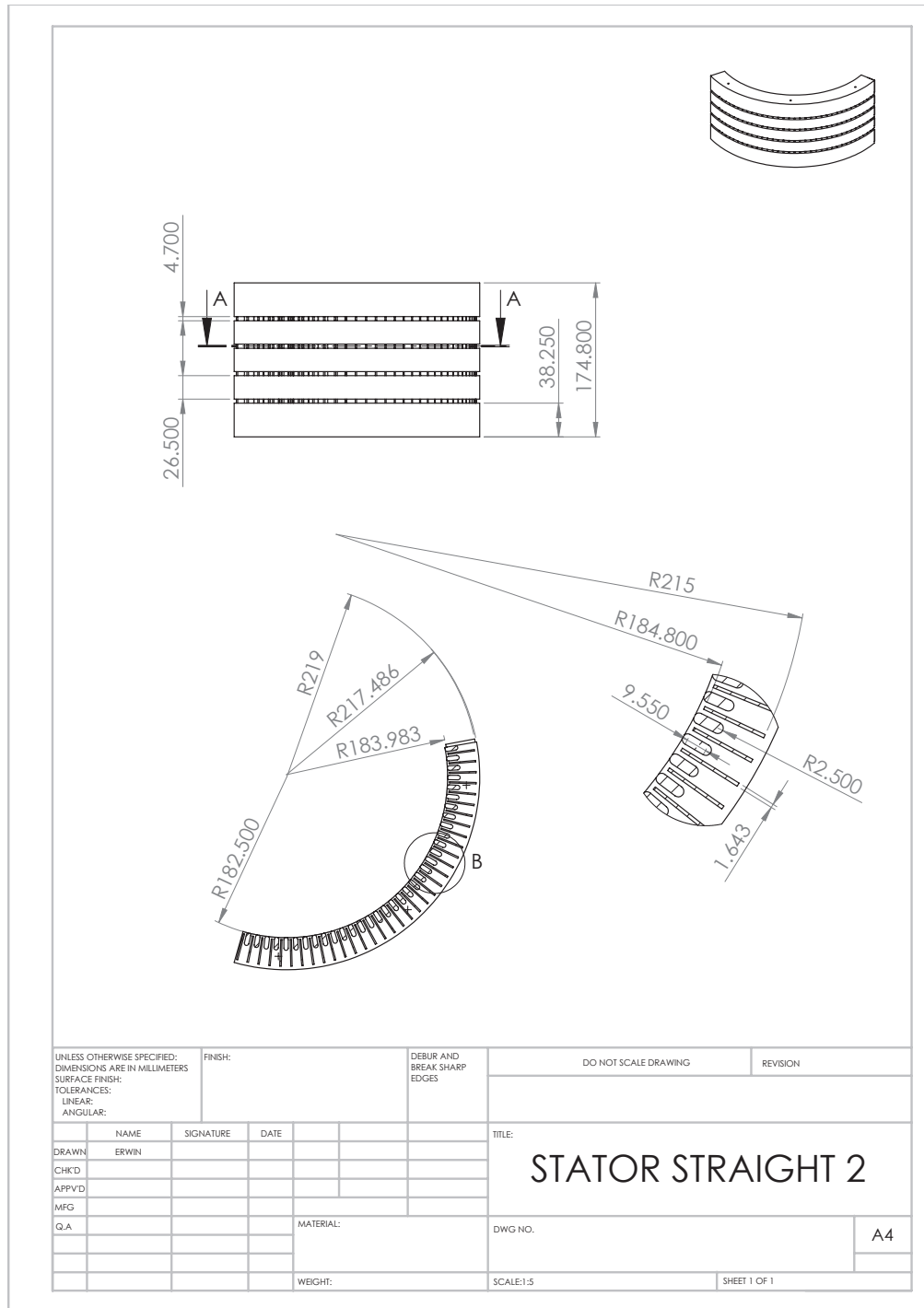
B.4 Stator Curved Baffles 3 of 3



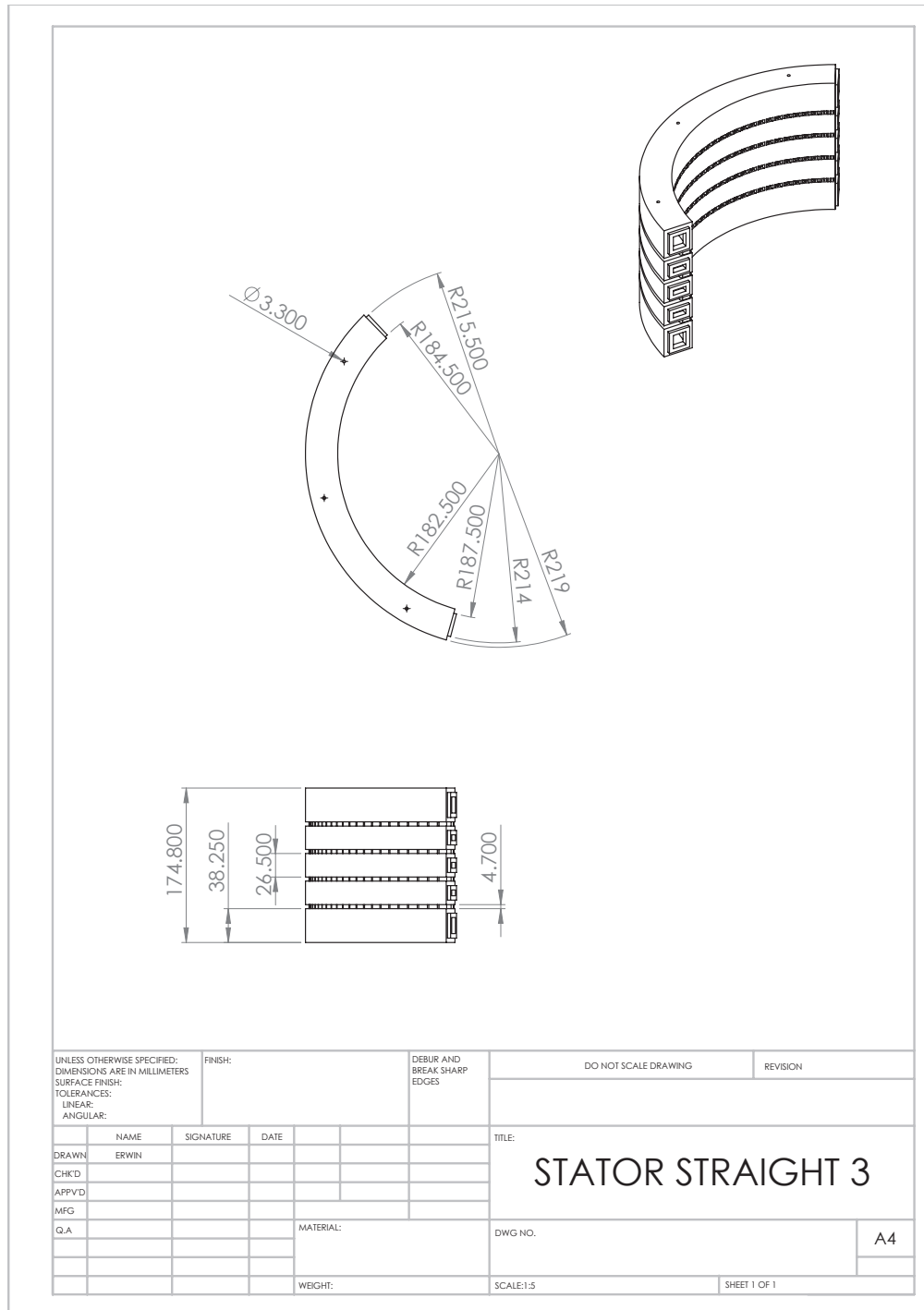
B.5 Stator Straight Baffles 1 of 3



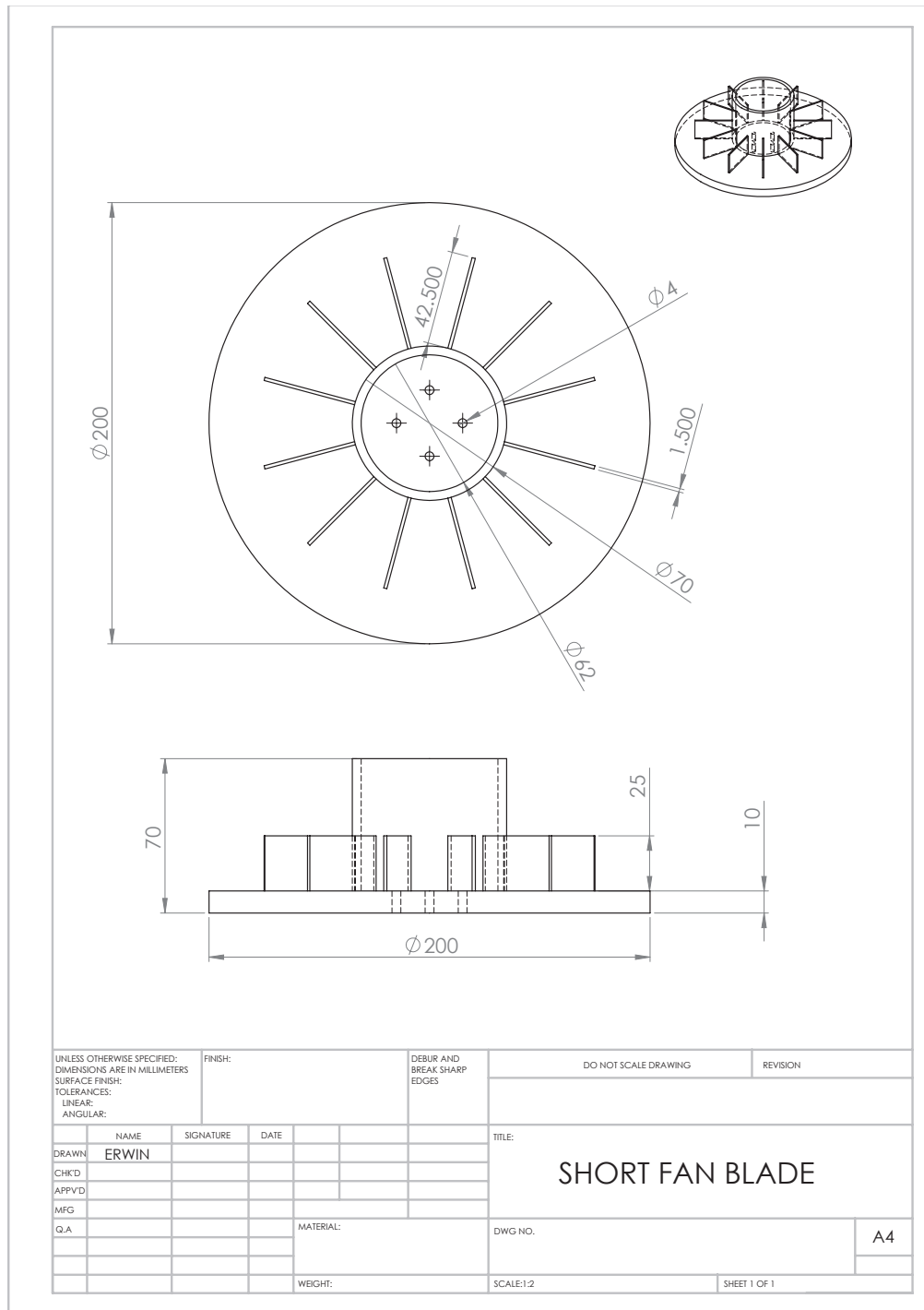
B.6 Stator Straight Baffles 2 of 3



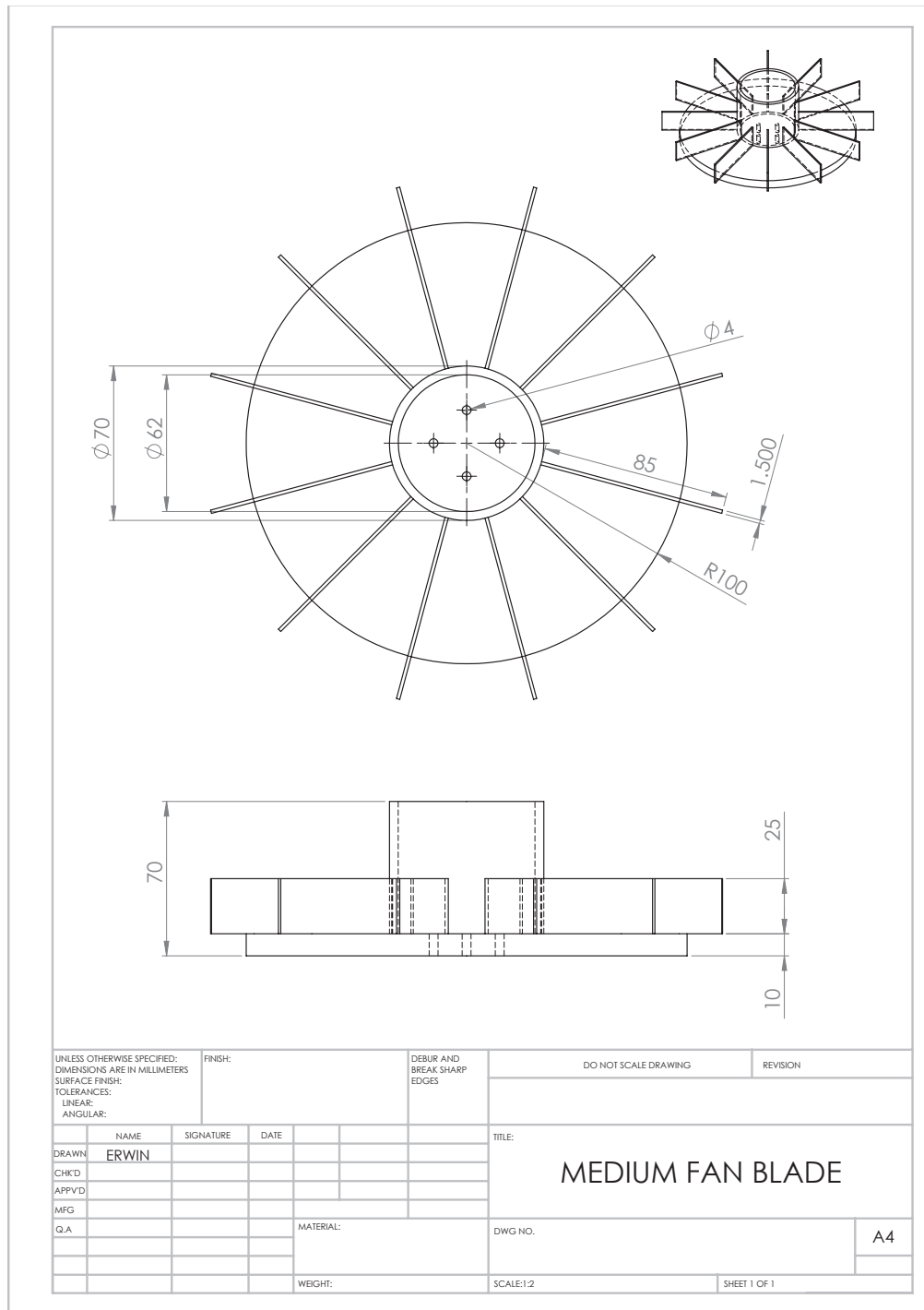
B.7 Stator Straight Baffles 3 of 3



B.8 Short fan blade



B.9 Medium fan blade



B.10 Long fan blade

